

The Photophysical Properties of Quaternary Lanthanide (Eu^{3+} , Tb^{3+} , Sm^{3+} , Dy^{3+}) Functional Molecular Complexes

Bing Yan* and Qiyu Xie

Department of Chemistry, Tongji University, Shanghai 200092, China

Received November 10, 2003; accepted (revised) January 8, 2004

Published online April 22, 2004 © Springer-Verlag 2004

Summary. In this paper, according to the molecular fragment principle, a series of twelve quaternary luminescent lanthanide complex molecular systems were assembled. Both elemental analysis and infrared spectroscopy allowed to determine the complexes formula: $\text{Ln}(\text{Nic})_3(\text{L})\cdot\text{H}_2\text{O}$, where $\text{Ln} = \text{Sm}, \text{Eu}, \text{Tb}, \text{Dy}$; $\text{HNic} = \text{pyridine-3-carboxylic acid}$; $\text{L} = \text{N,N-dimethylformamide (DMF)}$, $\text{N,N-dimethylacetamide (DMA)}$, $\text{pyrrolidone (pyro)}$. The photophysical properties of these functional molecular systems were studied by recording both ultraviolet-visible absorption, phosphorescence, fluorescence excitation, and emission spectra. It was found that the conjugated pyridine-3-carboxylic acid acts as the main energy donor and luminescence sensitizer due to the suitable energy match and effective energy transfer to the luminescent Ln^{3+} ions. Amide molecules (DMF , DMA , pyro) were only used as assistant structural ligands to enhance the luminescence. Especially the europium complexes show the strongest luminescence due to the optimum energy transfer between the HNic triplet state energy level and Eu^{3+} .

Keywords. Molecular fragment principle; Molecular assembly; Quaternary lanthanide functional molecular complexes; Photophysical properties.

Introduction

The photophysical properties of lanthanide coordination compounds with organic ligands have been the subject of great interest because these functional complex systems show potential applications such as the active center of luminescent materials [1–3] or as structural and functional probe for chemical and biological macromolecular systems [4–6]. A variety of research was reported on the energy transfer and luminescence of lanthanide complexes with β -diketones or aromatic carboxylic acids, which show good energy levels match and, afterwards good

* Corresponding author. E-mail: byan@tongji.edu.cn

luminescent properties of lanthanide ions [7–10]. We also have studied the energy match and intramolecular energy transfer mechanism of binary and ternary lanthanide complexes with aromatic carboxylic acids and 1,10-phenanthroline in details [11–14]. In the context, using a conjugated carboxylic acid (pyridine-3-carboxylic acid) as the energy donor and luminescence sensitizer of lanthanide ions and amide molecules as the second or the third assistant structural ligands, a series of twelve quaternary lanthanide (Eu^{3+} , Tb^{3+} , Sm^{3+} , Dy^{3+}) complex systems was assembled. The corresponding photophysical properties were studied in detail in this paper.

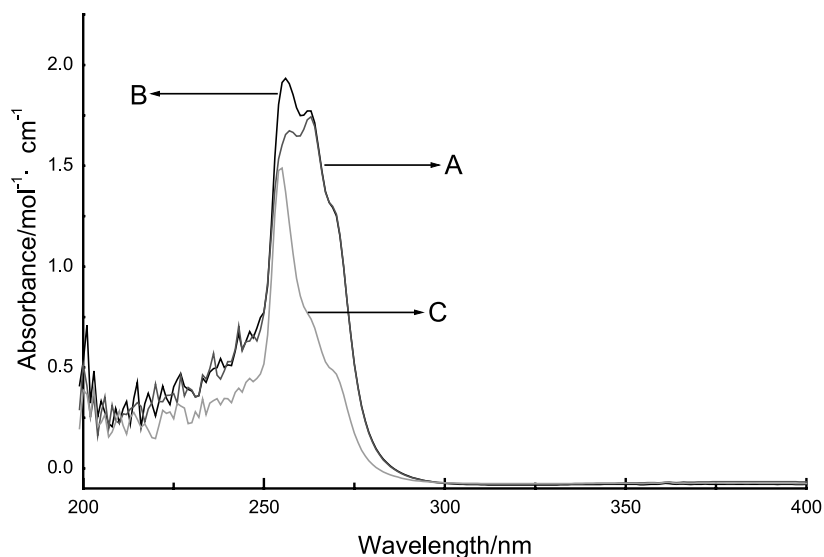
Results and Discussion

The composition of the complex systems was confirmed by chemical analyses and leads to $\text{Ln}(\text{HNic})_3(L) \cdot \text{H}_2\text{O}$, ($\text{Ln} = \text{Sm}, \text{Eu}, \text{Tb}, \text{Dy}$; $\text{HNic} = \text{pyridine-3-carboxylic acid}$; $L = \text{N,N-dimethylformamide (DMF)}$, $\text{N,N-dimethylacetamide (DMA)}$, $\text{pyrrolidone (pyro)}$). All IR spectra of these molecular systems show similar features. For $\text{Eu}(\text{Nic})_3(\text{DMF}) \cdot \text{H}_2\text{O}$ complex, characteristic absorption bands of $\text{C}=\text{O}$ (1710 cm^{-1}) and $\text{C}-\text{O}$ (1344 cm^{-1}) belonging to the free ligand (HNic) disappear, while the characteristic absorption peaks of a carboxylic group COO^- appear (1412 cm^{-1} , 1555 cm^{-1}), which suggest that the oxygen atom of pyridine-3-carboxylic acid's carboxylate group is coordinated with Eu^{3+} . The $\text{C}-\text{O}$ stretching vibration frequency of amide group shifts from high wavenumber (1676 cm^{-1}) for free DMF to a lower value of 1600 cm^{-1} for complexes, indicating that DMF is coordinated with Eu^{3+} . In the same way, for $\text{Tb}(\text{Nic})_3(\text{DMA}) \cdot \text{H}_2\text{O}$ systems, $\text{C}-\text{O}$ stretching vibration frequency of the amide group of DMA shifts from high wavenumber (1676 cm^{-1}) for free DMA to a lower value of 1600 cm^{-1} for complexes, indicating that Tb^{3+} is coordinated by DMA . For $\text{Tb}(\text{Nic})_3(\text{pyro}) \cdot \text{H}_2\text{O}$ systems, absorption bands of the carboxylate group show the similar features as those of $\text{Tb}(\text{Nic})_3(\text{DMF})_2 \cdot \text{H}_2\text{O}$. Moreover, $\text{C}-\text{O}$ stretching vibration frequency of the amide group of pyro shifts from high wavenumber (1676 cm^{-1}) for free pyro to a lower value of 1600 cm^{-1} for complexes, indicating that Tb^{3+} is coordinated by pyro . Besides, it can be observed that the absorption frequency of $\text{Ln}-\text{O}$ bond lies at about $\bar{\nu} = 419 \text{ cm}^{-1}$. Some other apparent bands are noted at about $\bar{\nu} = 3450$ and 1613 cm^{-1} , which are respectively attributed to the stretching vibration and in-plane bending of H_2O molecules. The absorption bands corresponding to the in-plane swing vibration of coordinated H_2O molecules have not been observed in the range of $\bar{\nu} = 605 \sim 585 \text{ cm}^{-1}$, which verifies that the water molecule is not coordinated to the lanthanide ion and, thus, corresponds to a crystal water molecule [15]. Other $\text{Ln}(\text{Nic})_3(L) \cdot \text{H}_2\text{O}$ complex systems show similar features. Table 1 gives the detailed data for the main absorption bands and assignments.

Figure 1 shows the representative ultraviolet absorption spectra for $\text{Eu}(\text{Nic})_3(\text{DMF}) \cdot \text{H}_2\text{O}$ (A), $\text{Tb}(\text{Nic})_3(\text{DMA}) \cdot \text{H}_2\text{O}$ (B), and $\text{Dy}(\text{Nic})_3(\text{pyro}) \cdot \text{H}_2\text{O}$ (C), respectively. $\text{Eu}(\text{Nic})_3(\text{DMF}) \cdot \text{H}_2\text{O}$ shows two main absorption peaks at about 257 and 263 nm and a shoulder near 275 nm. The $\text{Tb}(\text{Nic})_3(\text{DMA}) \cdot \text{H}_2\text{O}$ complex also exhibits two main absorption peaks at about 256 and 263 nm and a shoulder near 275 nm. One absorption peak at 255 nm and two shoulders at 263 and 273 nm can be observed in the absorption spectrum of $\text{Dy}(\text{Nic})_3(\text{DMA}) \cdot \text{H}_2\text{O}$. The absorption bands at 257 (257, 255) nm and 273 nm can be attributed to the characteristic absorption of

Table 1. The IR absorption bands of $Ln-Nic-L \cdot H_2O$ molecular systems

Complex systems	$\bar{\nu}_{S,COO^-}/cm^{-1}$	$\bar{\nu}_{aS,COO^-}/cm^{-1}$	$\bar{\nu}_{S,C-O-NH}/cm^{-1}$	$\bar{\nu}_{H_2O}/cm^{-1}$
$Eu(Nic)_3(DMF) \cdot H_2O$	1412	1555	1600	3455, 1613
$Tb(Nic)_3(DMF) \cdot H_2O$	1412	1554	1600	3455, 1613
$Sm(Nic)_3(DMF) \cdot H_2O$	1412	1555	1600	3455, 1613
$Dy(Nic)_3(DMF) \cdot H_2O$	1412	1555	1600	3449, 1613
$Eu(Nic)_3(DMA) \cdot H_2O$	1418	1555	1600	3417, 1613
$Tb(Nic)_3(DMA) \cdot H_2O$	1418	1555	1600	3423, 1613
$Sm(Nic)_3(DMA) \cdot H_2O$	1418	1555	1600	3410, 1613
$Dy(Nic)_3(DMA) \cdot H_2O$	1418	1555	1600	3423, 1613
$Eu(Nic)_3(pyro) \cdot H_2O$	1412	1555	1600	3423, 1613
$Tb(Nic)_3(pyro) \cdot H_2O$	1412	1555	1600	3423, 1613
$Sm(Nic)_3(pyro) \cdot H_2O$	1412	1555	1600	3417, 1613
$Dy(Nic)_3(pyro) \cdot H_2O$	1412	1555	1600	3410, 1613

**Fig. 1.** Ultraviolet absorption spectra of $Eu(Nic)_3(DMF) \cdot H_2O$ (A), $Tb(Nic)_3(DMA) \cdot H_2O$ (B), and $Dy(Nic)_3(pyro) \cdot H_2O$ (C)

the $HNic$ ligand and the absorption bands at around 263 nm correspond to the amide group. The absorption band of $Dy(Nic)_3(pyro) \cdot H_2O$ (C) shows some difference from the that of $Eu(Nic)_3(DMF) \cdot H_2O$ (A) and $Tb(Nic)_3(DMA) \cdot H_2O$ (B), which is due to that $pyro$ has a pyrrole heterocycle different from the another two amide groups (DMF and DMA). The results indicate that $HNic$ is the main energy donor and luminescence sensitizer for Ln^{3+} ion. Other ultraviolet absorption spectra show similar features. According to the intramolecular energy transfer mechanism, the luminescent property of lanthanide complexes mainly depends on the energy match between the triplet state energy of ligands and the resonance emission energy level of lanthanide ions [11–13]. So we measured the low temperature phosphorescence of $Gd(Nic)_3(H_2O)_2$ and determined the triplet state energy of $HNic$ (as shown in Fig. 2).

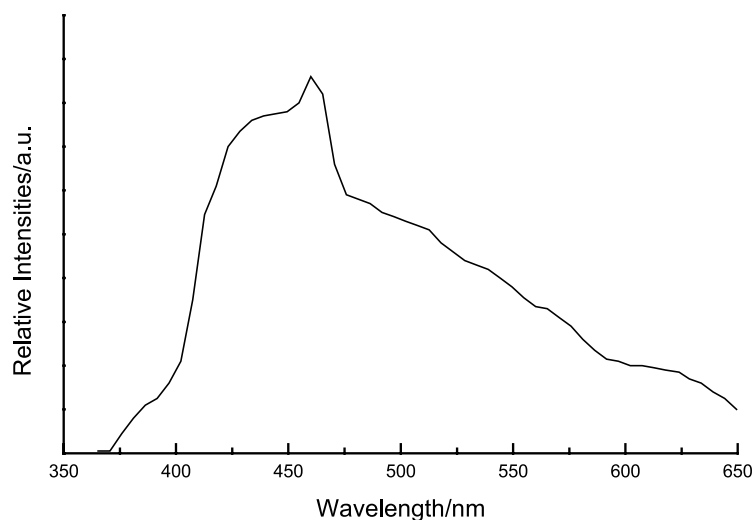


Fig. 2. Phosphorescence spectrum of $\text{Gd}(\text{Nic})_3 \cdot \text{H}_2\text{O}$ complex

It can be seen that the phosphorescence band is centered at around 460 nm and the triplet state energy of *HNic* can be estimated to be 21740 cm^{-1} . The energy differences between the triplet state of *HNic* and the resonance energy level of Eu^{3+} ($^5\text{D}_0$, 17600 cm^{-1}), Tb^{3+} ($^5\text{D}_4$, 20500 cm^{-1}), Sm^{3+} ($^4\text{G}_{5/2}$, 17900 cm^{-1}), and Dy^{3+} ($^4\text{F}_{9/2}$, 21000 cm^{-1}) can be calculated to be 4140, 1240, 3840, and 740 cm^{-1} , respectively. From these energy differences, it can be predicted that *HNic* ligand is more suitable for the sensitization of Eu^{3+} ion's luminescence than other Ln^{3+} [11–14].

The excitation spectra of these complex systems show that there is no effective absorption in the 300–400 nm ultraviolet region. Figure 3 gives the excitation spectrum of $\text{Eu}(\text{Nic})_3(\text{DMF}) \cdot \text{H}_2\text{O}$. The effective energy absorption mainly takes

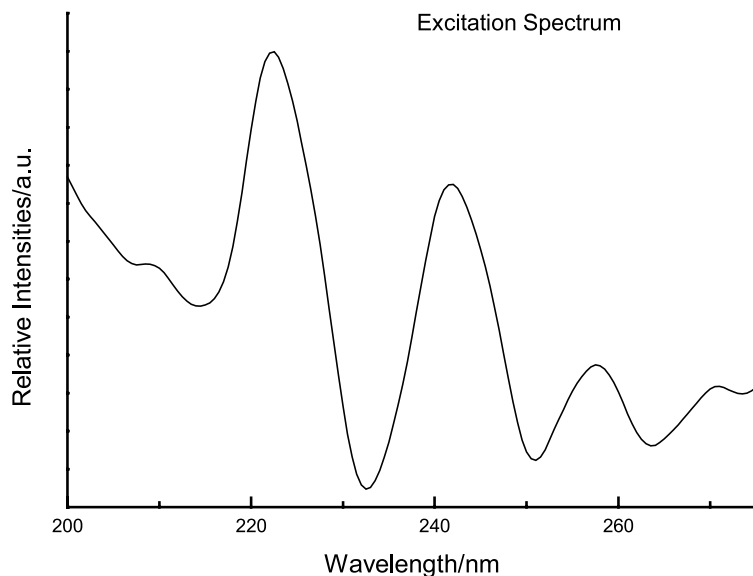


Fig. 3. Excitation spectrum of $\text{Tb}(\text{Nic})_3(\text{DMA}) \cdot \text{H}_2\text{O}$ complex

place in the narrow ultraviolet region of 200–280 nm. Four main excitation bands are located at 222, 242, 257, and 271 nm, respectively. We further measured the corresponding emission spectra by selective excitation into the four different components; they show a similar emission position except for different luminescent intensities. This indicates that excitation into the four bands (Fig. 3) allows an effective energy sensitization for the luminescence of Ln ions.

The emission spectra were measured in detail. Figs. 4, 5, and 6 give the selected emission spectra of $\text{Eu}(\text{Nic})_3(\text{DMA}) \cdot \text{H}_2\text{O}$, $\text{Tb}(\text{Nic})_3(\text{DMF}) \cdot \text{H}_2\text{O}$, and

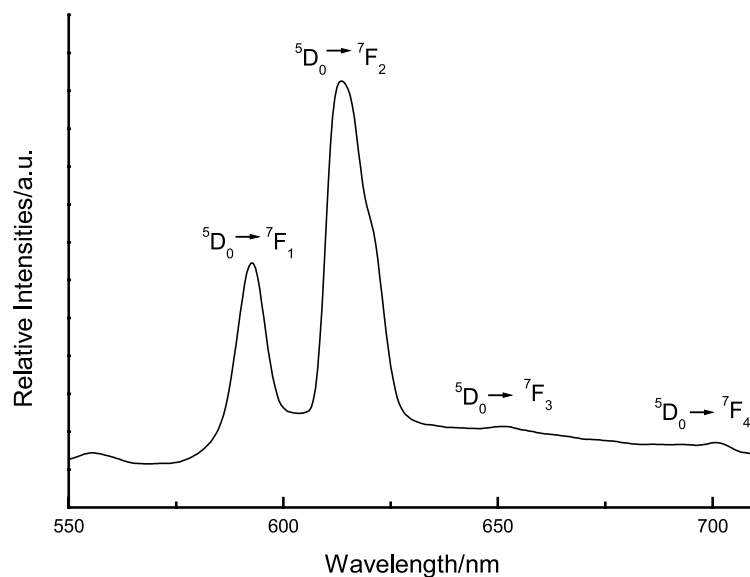


Fig. 4. Emission spectrum of $\text{Eu}(\text{Nic})_3(\text{DMA}) \cdot \text{H}_2\text{O}$ complex ($\lambda_{\text{ex}} = 241$ nm)

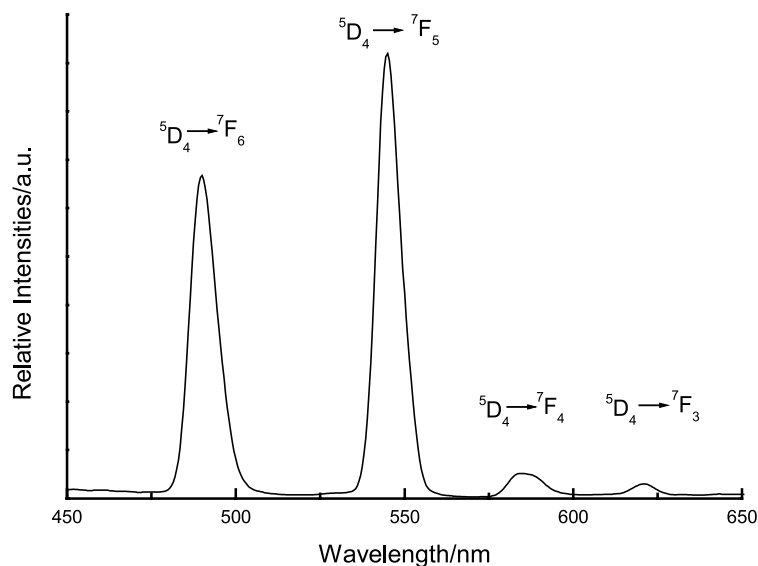


Fig. 5. Emission spectrum of $\text{Tb}(\text{Nic})_3(\text{DMF}) \cdot \text{H}_2\text{O}$ complex ($\lambda_{\text{ex}} = 241$ nm)

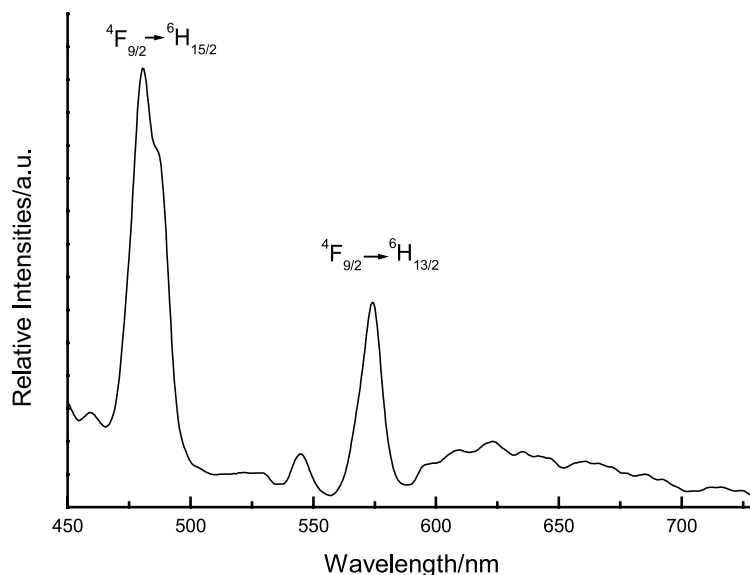


Fig. 6. Emission spectrum of $\text{Dy}(\text{Nic})_3(\text{pyro}) \cdot \text{H}_2\text{O}$ complex ($\lambda_{\text{ex}} = 241 \text{ nm}$)

$\text{Dy}(\text{Nic})_3(\text{DMF}) \cdot \text{H}_2\text{O}$, respectively. For $\text{Eu}(\text{Nic})_3(\text{DMA}) \cdot \text{H}_2\text{O}$ complex, the emission spectrum shows four emission peaks under excitation at 242 nm: 592.4, 618.2, 651.8, and 698.5 nm, corresponding to the characteristic ${}^5\text{D}_0 \rightarrow {}^7\text{F}_j$ emission transitions ($j = 1, 2, 3, 4$) of Eu^{3+} ion. The ${}^5\text{D}_0 \rightarrow {}^7\text{F}_2$ emission intensity is the greatest one, leading to a strong red luminescence; the ${}^5\text{D}_0 \rightarrow {}^7\text{F}_1$ transition is large enough to cover the ${}^5\text{D}_0 \rightarrow {}^7\text{F}_0$ transition. For $\text{Tb}(\text{Nic})_3(\text{DMF}) \cdot \text{H}_2\text{O}$ complex, the emission spectrum shows four emission peaks under excitation at 223 nm: 490.3, 544.4, 583.9, and 621.0 nm, attributed to the characteristic ${}^5\text{D}_4 \rightarrow {}^7\text{F}_j$ ($j = 6, 5, 4, 3$) emission transitions of Tb^{3+} ion. Among them, the ${}^5\text{D}_4 \rightarrow {}^7\text{F}_5$ transition exhibits the strongest emission (in the green region), and ${}^5\text{D}_4 \rightarrow {}^7\text{F}_6$ transition shows the second strongest emission (in the blue region). For $\text{Dy}(\text{Nic})_3(\text{pyro}) \cdot \text{H}_2\text{O}$ complex, the luminescence spectrum shows two apparent emission peaks under excitation at 238 nm: one is located at 483.9 nm and the other at 574.2 nm; they correspond respectively to the characteristic ${}^4\text{F}_{9/2} \rightarrow {}^6\text{H}_j$ ($j = 15/2, 13/2$) emission transitions of Dy^{3+} ion. It is worthy pointing out that the blue emission intensity of ${}^4\text{F}_{9/2} \rightarrow {}^6\text{H}_{15/2}$ transition is stronger than the yellow emission of ${}^4\text{F}_{9/2} \rightarrow {}^6\text{H}_{13/2}$, suggesting that the nicotinic acid is suitable for the sensitization of Dy^{3+} blue luminescence in $\text{Dy}(\text{Nic})_3(\text{pyro}) \cdot \text{H}_2\text{O}$ complex. Other lanthanide complex systems (Eu^{3+} , Tb^{3+} , Dy^{3+}) show similar features.

All the samarium complex systems show no ideal luminescence spectra. Comparing the luminescence intensities of these complex systems, it can be found that quaternary europium complex systems show a stronger luminescence than that observed for other lanthanide systems. The quaternary terbium and dysprosium complex systems show weaker luminescence than europium ones but stronger than samarium ones, which indicate that the triplet state energy is more suitable for the luminescence of europium ion than terbium and dysprosium ions. There exists some internal energy levels (${}^6\text{F}_{11/2}$, ${}^6\text{F}_{9/2}$, \dots , ${}^6\text{H}_{11/2}$, *etc.*) between the first

excited state ${}^4G_{5/2}$ and ground state ${}^6H_{9/2}$ of Sm^{3+} , which cause readily some non-radiative de-excitations from ${}^4G_{5/2}$ to a lot of lower energy levels (internal energy levels). So Sm^{3+} complex systems exhibit the weakest luminescence.

In summary, a series of lanthanide (Eu, Tb, Sm, Dy)-pyridine-3-carboxylic acid (HNic) – *L* (DMF, DMA, pyro) – H₂O quaternary complex systems have been synthesized and characterized. The photophysical properties of these systems have been studied with ultraviolet, excitation, and emission spectra. In these systems, the pyridine-3-carboxylic acid showing a conjugated structure acts as the main energy donor and sensitizes the luminescence of lanthanide ions. The second ligands, amide ligands (DMF, DMA, pyro), are used to complete the Ln³⁺ coordination sphere and thus to exclude coordinated water molecules, which behave as assistant structural ligands to influence the energy transfer process and luminescence in these quaternary systems. Among these systems, quaternary europium complexes exhibit the strongest luminescence.

Experimental

The lanthanide oxides (Eu₂O₃, Tb₄O₇, Sm₂O₃, Dy₂O₃) were converted to their nitrates by treatment with concentrated nitric acid. The quaternary lanthanide complexes were prepared by homogeneous precipitation. DMF (DMA, pyro) solutions of lanthanide nitrates were added very slowly to the DMF (DMA, pyro) solutions of HNic. The pH value of the mixed DMF (DMA, pyro) solutions was adjusted to about 6.5 using sodium hydroxide. Then white precipitates appeared and were filtered off, washed with DMF (DMA, pyro), dried, and stored over silica gel.

Elemental analysis (C, H, N) was carried out by an Elementar Carlo EL elemental analyzer; results were in agreement with calculated values. Infrared spectroscopy on KBr pellets was performed on a Nicolet Nexus 912 AO446 model spectrophotometer in the range of $\bar{\nu} = 4000 \sim 400 \text{ cm}^{-1}$. Ultraviolet absorption spectra of these complexes ($5 \times 10^{-4} \text{ M}$ ethanol solution) were recorded with an Agilent 8453 spectrophotometer. Luminescence (excitation and emission) spectra of these solid complexes and phosphorescence spectrum of Gd(Nic)₃(H₂O)₂ complex ($5 \times 10^{-4} \text{ M}$ ethanol solution) was determined with a Perkin-Elmer LS-55 spectrophotometer whose excitation and emission slits were 10 and 5 nm, respectively.

Acknowledgements

This work was supported by the Start Science Fund of Tongji University for Talents.

References

- [1] Yan B, Zhang HJ, Wang SB, Ni JZ (1997) Mater Chem Phys **51**: 92
- [2] Yan B, Zhang HJ, Wang SB, Ni JZ (1998) Mater Res Bull **33**: 1517
- [3] Yan B, Zhang HJ, Ni JZ (1997) Mater Sci Eng **B59**: 123
- [4] Meares CF, Wensel TG (1984) Acc Chem Res **17**: 202
- [5] Ci YX, Li YZ, Chang WB (1991) Anal Chim Acta **248**: 589
- [6] Scott LK, Horrocks WD (1994) J Inorg Biochem **46**: 193
- [7] Yang YS, Gong ML, Li YY, Lei HY, Wu SL (1994) J Alloys Compds **207/208**: 112
- [8] Wan YH, Jin LP, Wang KZ (2003) J Mol Struct **649**: 85
- [9] Feng CJ, Luo QH, Duan CY (1998) J Chem Soc, Dalton Trans 377
- [10] Yan B, Zhang HJ, Wang SB, Ni JZ (1998) J Photochem Photobiol, A Chem **116**: 209
- [11] Yan B, Zhang HJ, Wang SB, Ni JZ (1998) Spectros Lett **31**: 603

- [12] Yan B, Zhang HJ, Wang SB, Ni JZ (1998) Chem Pap **52**: 199
- [13] Yan B, Zhang HJ, Wang SB, Ni JZ (1998) Monatsh Chem **129**: 151
- [14] Yan B, Zhang HJ, Wang SB, Ni JZ (1998) Monatsh Chem **129**: 567
- [15] Ma AZ, Li LM, Xi SQ (1993) Chin J Anal Chem **21**: 105